

X-RAY SPECTROMETRY OF GALACTIC SOURCES IN THE ENERGY RANGE 30–200 keV

A. BUI-VAN, G. VEDRENNE, and Y. CEZAC

Centre d'Etude Spatiale des Rayonnements, Toulouse, France

and

A. BOUIGUE and L. SABAUD

Observatoire de Toulouse, Toulouse, France

Abstract. We describe a detection unit for X-rays in the energy range 30–200 keV of high directivity (2° FWHM). This directivity is obtained by the use of a honeycomb collimator and completed by an efficient passive shielding. The angular resolution of the detector necessitates the use of a solar sensor so as to track the sources observed during the balloon flight and to localize them with an accuracy of 3.8 arc min. This experiment was launched with balloon at Aire-sur-L'Adour and Gap (France) and the results obtained must permit the flux limit detected to be reduced.

The performances of this detector are analysed as well as their consequences in the study of galactic discrete sources.

1. Introduction

As the fluxes emitted by X-ray sources are weak compared with the surrounding background, one solution for increasing the signal to noise ratio of the detection system is to improve its angular resolution. This can be obtained by associating it with a honeycomb collimator. Furthermore this solution could provide more detailed information as to the position and angular size of the discrete sources.

At balloon altitudes the detection system is exposed to the full flux of galactic and atmospheric cosmic rays. These highly interacting particles are efficient for producing photons if passive shieldings are employed to protect the detector from X-rays outside the aperture angle (Peterson *et al.*, 1967; Bleeker *et al.*, 1970; Brini *et al.*, 1967; Haymes *et al.*, 1969). However, as this type of shielding is not so expensive as the active ones, it has been used in designing the X-ray telescope. We have perfected this telescope by striving at the same time as we increased the angular resolution of the device ($\sim 2^\circ$ FWHM) to obtain as weak a contribution as possible of the X-ray background produced in the detector by cosmic rays and by the scattering of high energy gamma rays. We are going to describe the experimental system and some results concerning balloon launchings from Gap and Aire-sur-L'Adour in France.

2. Instrumentation

The detector used at CESR is shown in Figure 1. It consists of a sandwich of thin Caesium Iodide crystal (0.2 cm thick) between two plastic scintillators. Its directivity is obtained by a passive honeycomb collimator and a passive shielding made with association of lead, tantalum and tin so that fluorescence of materials which appears

in the analysed energy range is rejected (Bui-Van and Vedrenne, 1969). The system is surrounded by a veto plastic counter (1 cm thick) for charged particles. Moreover events due to cosmic rays entering the forward aperture are anticoincided by a thin plastic scintillator. The energy resolution of the detector, measured with monochromatic γ -rays, is that typically obtained by scintillation counters at these

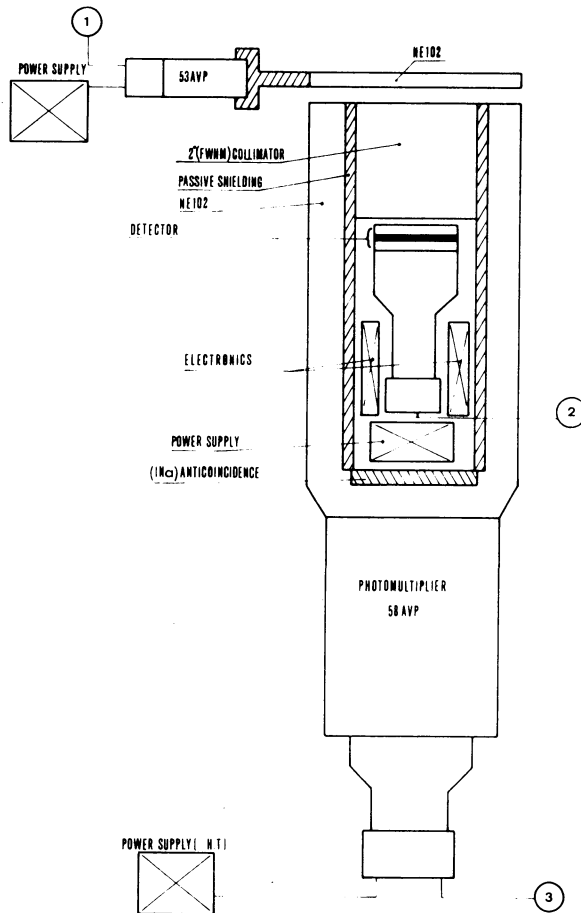


Fig. 1. Detector assembly.

energies, about 38% at 60 keV (^{241}Am). The geometrical half-flux angle of the collimator is tested at the laboratory. Calibration with radioactive sources gives the angular transmission and the value of the full width at half maximum is observed to be about 2° no matter what the γ -ray incidence energy (Figure 2). The modulation peak which appears at 7° angular incidence increases the geometrical factor of the instrument. Estimation of this factor gives $0.05 \text{ cm}^2 \text{ sr}$. for a detection area of 20 cm^2 . The electronic circuits associated with the detectors are shown in Figure 3.

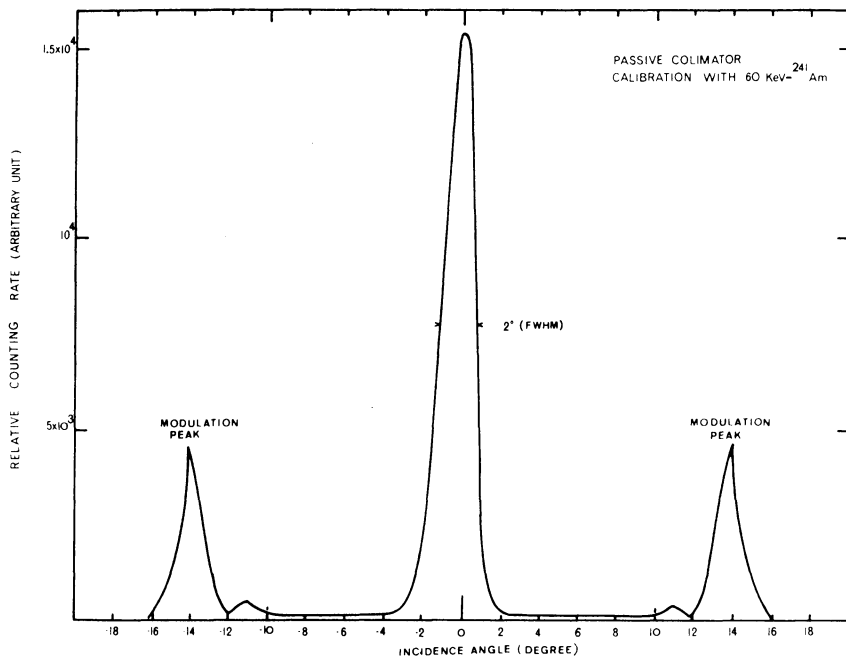


Fig. 2. Laboratory calibration of the passive honeycomb collimator.

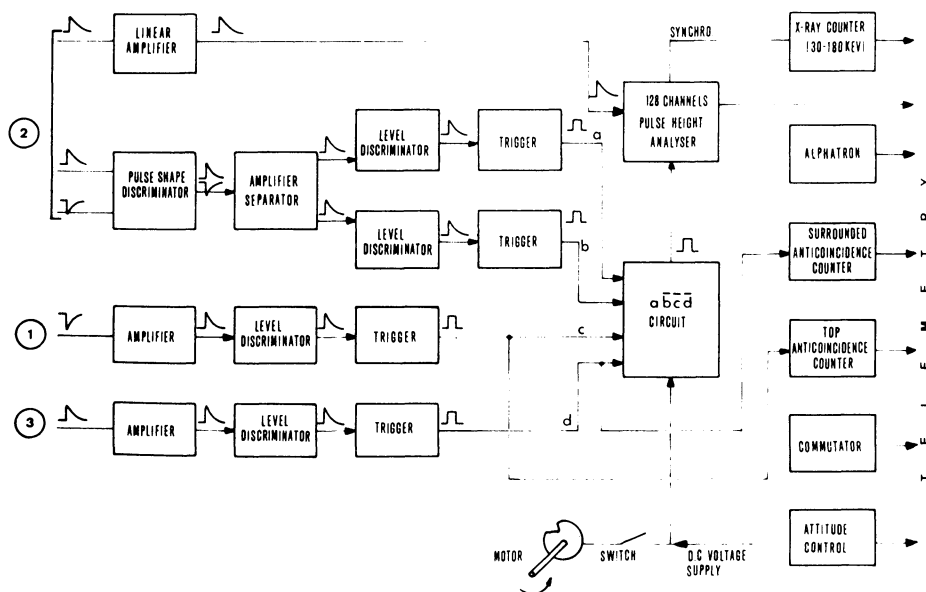


Fig. 3. Block-diagram of electronics circuits associated with the detector.

To allow the detector to aim at a fixed position on the celestial sphere, a tracking system is mounted on an oriented balloon payload. To provide orientation of this payload a compass sensor is fixed in the northern direction of the terrestrial magnetic field (Figure 4). A deviation of the azimuth angle caused by the balloon fastening or wind drift is then automatically corrected by gearing the inertia wheel. Tracking of the Sun during the diurnal motion is provided by an equatorial setting. The sensor unit for both the right ascension and the declination consists of a compensating circuit mounted with two symmetrical photocells. Sunbeams are collected on a prism which divides them perfectly into two rays (Figure 5). The resultant effect is such that when the Sun is not aimed a lack of balance exists in the circuit and contacts the reversible positioning motor. (Figure 6).

During the flight a programmed rotation of the experiment in a different direction from that of the source enables the intensity of the source and background to be compared.

To determine the accuracy of the orientation of the detector, a light tube is mounted parallel to the Sun sensors. A shaded film obscures in part the associated photocell. Its central transparent area transmits incident beams with less than $1^\circ 5'$ inclination. Thus the photocell gives an electrical signal which permits to estimate the position of the system axis with reference to the Sun.

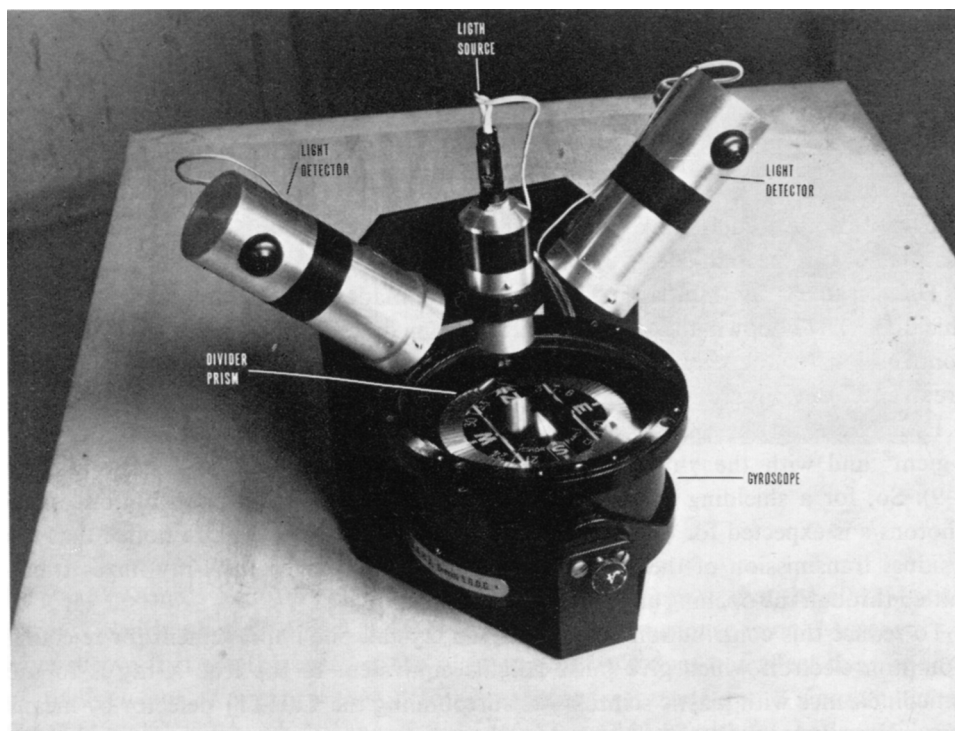


Fig. 4. Compass sensor associated with the azimuthal stabilisation.

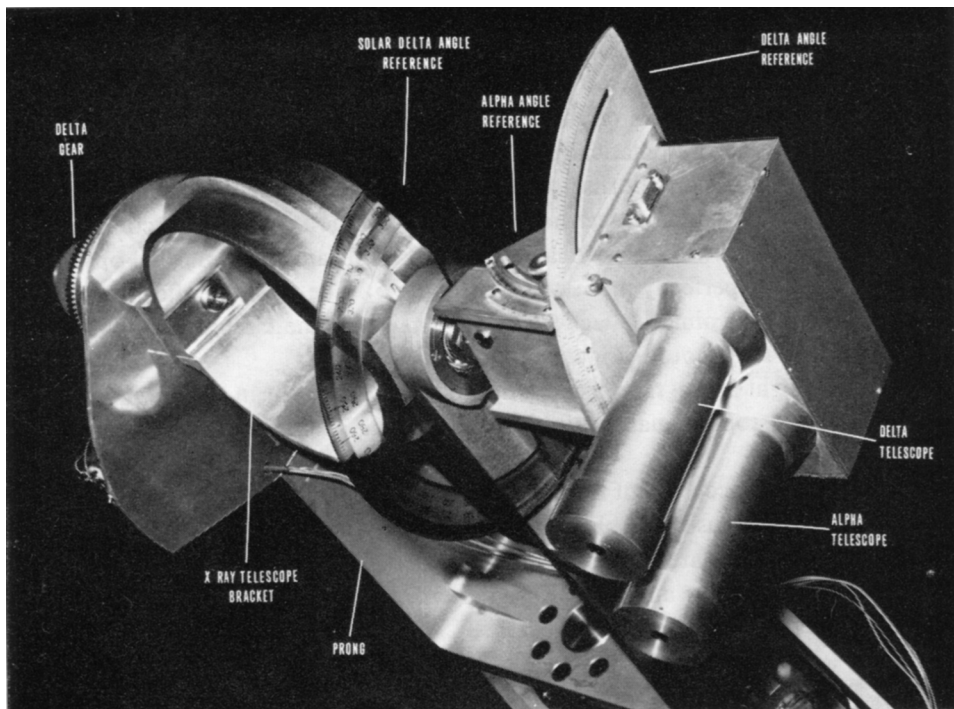


Fig. 5. Sensing units for right ascension and declination.

3. Results and Discussion

The laboratory studies have been intended to the evaluation of the background associated with the high-energy X-ray diffusion in the passive shielding.

Thanks to X-ray radioactive sources, tests made for different thicknesses of shieldings have shown that γ -rays emitted from different incidences give identical contributions to the background and that they do not increase when the thicknesses are over 0.7 cm (Figure 7).

Estimations on the diffusion contribution are calculated for a balloon altitude of 6 g/cm^2 and with the γ -ray flux expected, integrated between 0.2–2 MeV (Figure 8–9). So, for a shielding with a thickness of 0.5 cm, a residual contribution of 1.5 photons/s is expected for our detector. From this estimation, we can notice that the residual transmission of the shielding is very much higher than X-ray fluxes transmitted through the opening angle of the collimator.

To reduce this contribution in the analysed crystal, one improvement for rejecting Compton electron which give pulse heights equivalent to the true X-ray is to use anticoincidence with plastic scintillators surrounding the CsI(Tl) detector by means of a pulse shape discrimination circuit. The effect of rejection is simulated by high energy γ -ray sources which are put in front of the crystal unit during the irradiation

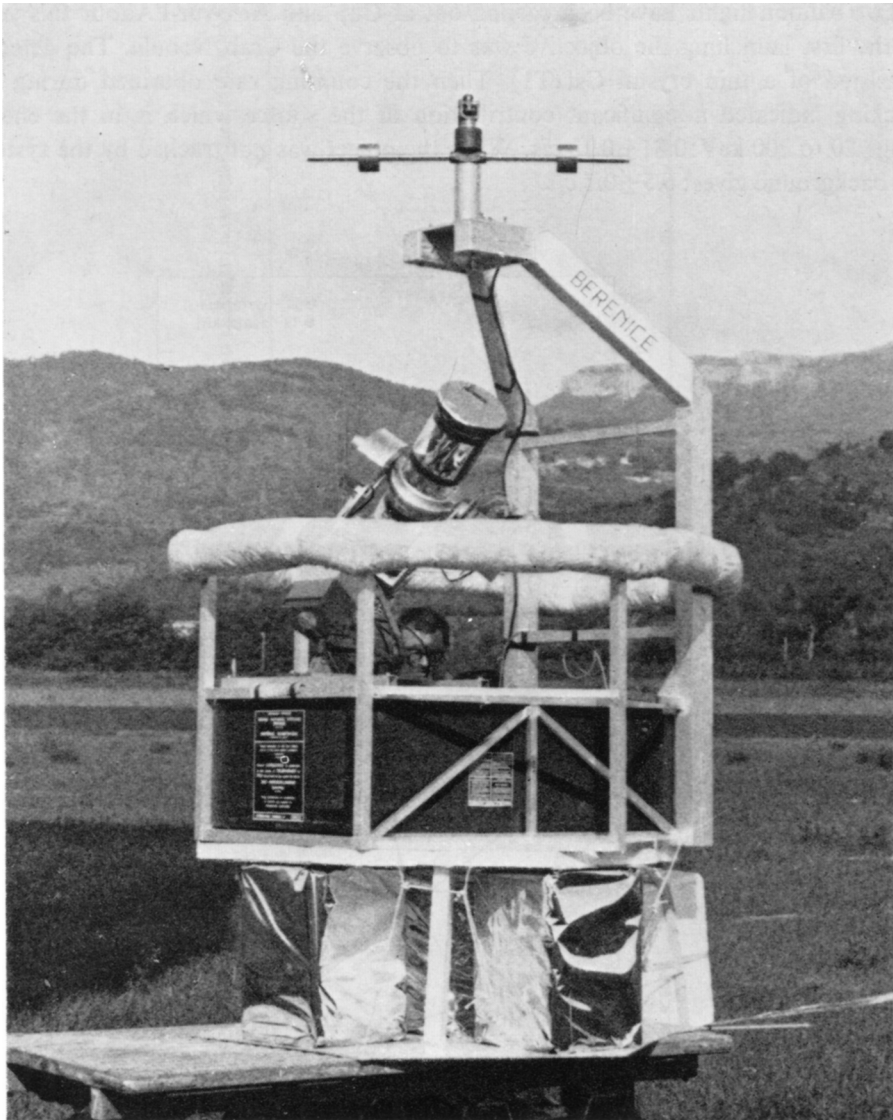


Fig. 6. Gondola on the launching area.

by 60 keV- Am^{241} X-ray (Figure 10). It is interesting to remark that the 60 keV-peak appears clearly above the background when the anticoincidence is on. Moreover we have shown that the thickness of the plastic scintillator does not affect the response of the detector. To prove this point comparison is made for 3 combinations: CsI(Tl) only; sandwich with anticoincidence; sandwich without anticoincidence (Figure 11). In no case does an energy shift appear in the position of X-ray lines.

Two balloon flights have been carried out at Gap and Aire-sur-l'Adour this year. In the first launching the objective was to observe the Crab Nebula. The detector consisted of a thin crystal CsI(Tl). Then the counting rate obtained during the tracking indicated a significant contribution of the source which is in the energy range 20 to 200 keV: 0.81 ± 0.13 c/s. When the object was not tracked by the system, the background gives: 6.5 ± 0.1 c/s.

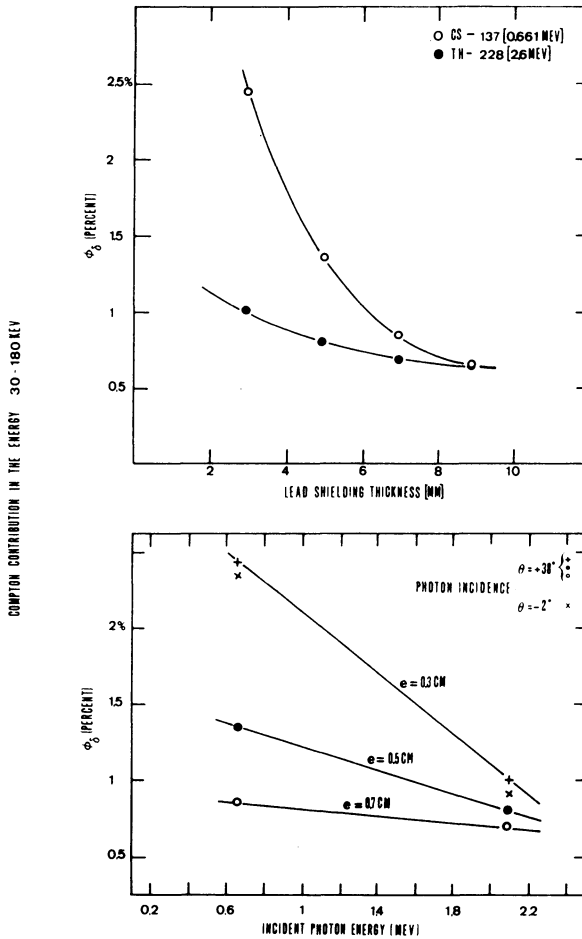


Fig. 7. High-energy γ -radioactive sources counting rate versus lead thickness.

In the second launching the Virgo region is surveyed. The sandwich detector employed gives a contribution of the source during the pointing: 0.51 ± 0.09 c/s, the corresponding background being: 6.13 ± 0.09 c/s (Figure 12). At the end of this flight an electronic switch authorized the inhibition of different anticoincidences. The

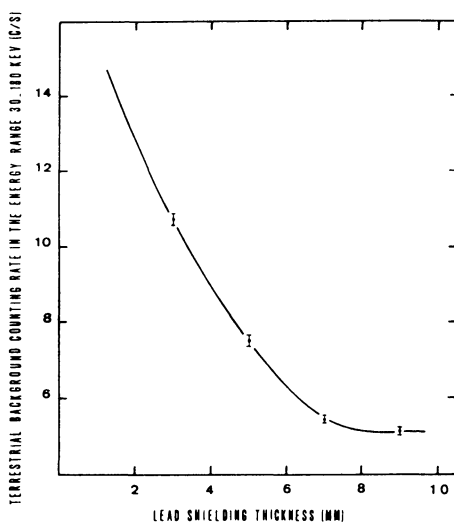


Fig. 8. High-energy terrestrial γ -ray counting rate versus lead thickness.

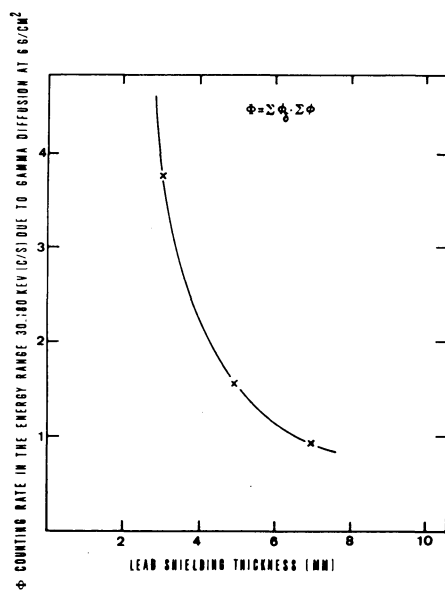


Fig. 9. γ -ray contribution at balloon altitude versus lead thickness.

counting rates obtained with and without anticoincidence permit the estimation of the rejection efficiencies which are:

- top anticoincidence: 50%
- surrounded anticoincidence: 60%
- sandwich detector anticoincidence: 10%

Finally, the main contributions to the counting rate obtained at the balloon altitude are:

residual transmission through a passive shielding 3.3 c/s
diffusion by high energy gamma-rays 1.5 c/s

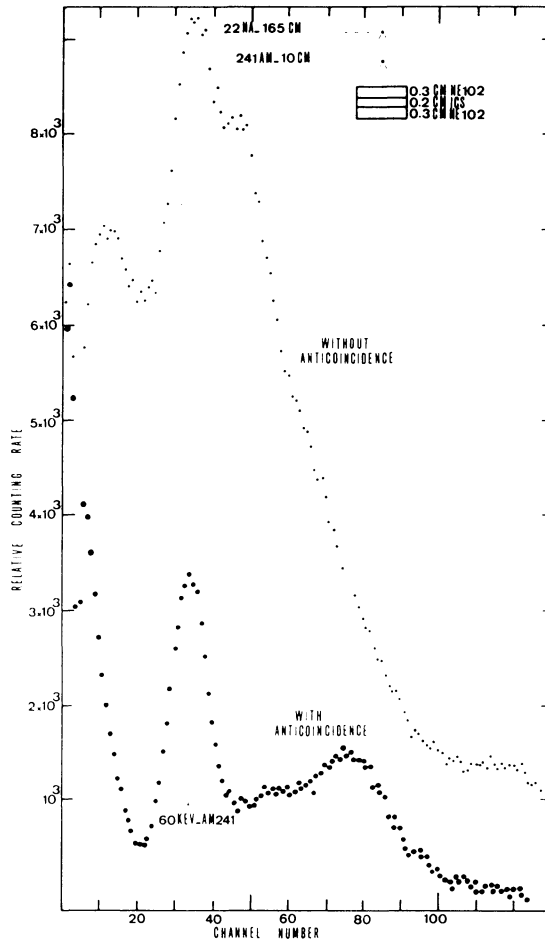


Fig. 10. Rejection effect of electrons emitted high-energy γ -ray.

The atmospheric and galactic flux through the collimator (0.06 c/s) is negligible compared with the two last contributions.

During these flights informations about the acquisition of the pointing system were transmitted. A continuous registration of the telemetry output allows the errors in the pointing and in the stabilisation to be obtained; according to the labor-

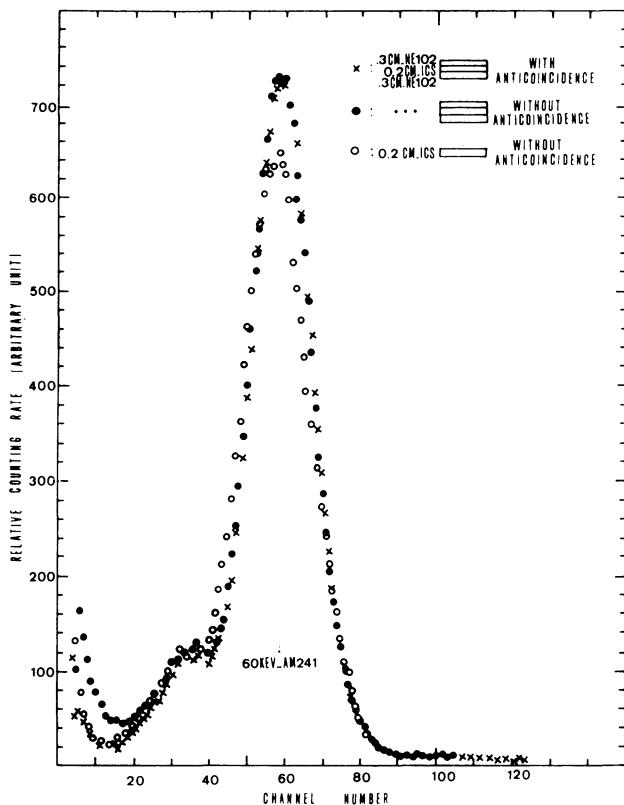


Fig. 11. Response of the sandwich detector.

atory calibration, the accuracy of the pointing is 6 arc min (Figure 13); and for the stabilisation 3.8 arc min (Figure 14).

4. Conclusion

In conclusion the two flights made with the detecting unit described here show mainly that the contribution of the background in the opening angle of the detector may be neglected compared with other contribution and particularly with the residual transmission and the high-energy γ diffusion in the shielding. Thus passive shielding cannot completely reject photons and the utilisation of an active shielding seems essential to reduce the lateral transmission. For instance if the detector is shielded by 2.7 cm CsI, the counting rate at 4.0 g/cm² is expected to be 1 c/s. But as the detected area is only 30% of the total area, the background of the detector in our experiment can be reduced by using a mosaic association of independant crystal CsI surrounded by a plastic gabarit. The background of the detector with this arrangement

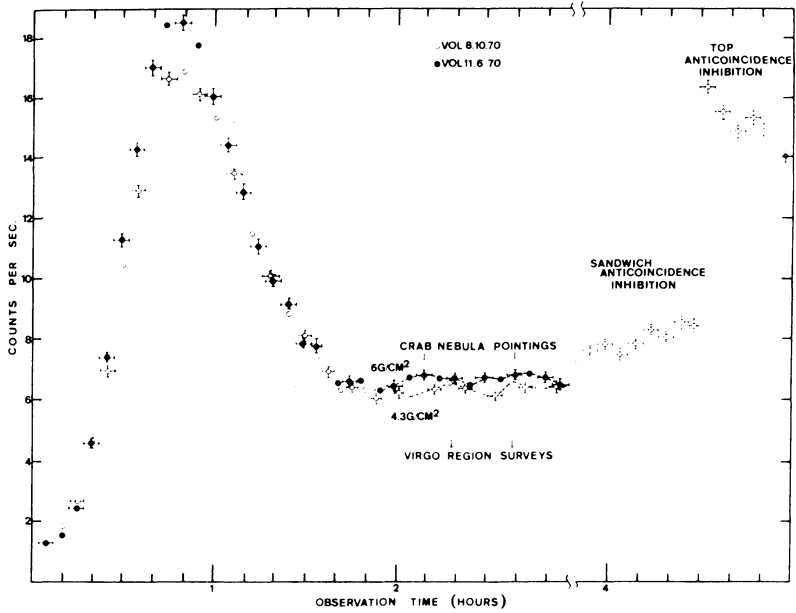


Fig. 12. Counting rates measured during the two observations made at Gap and Aire sur l'Adour.

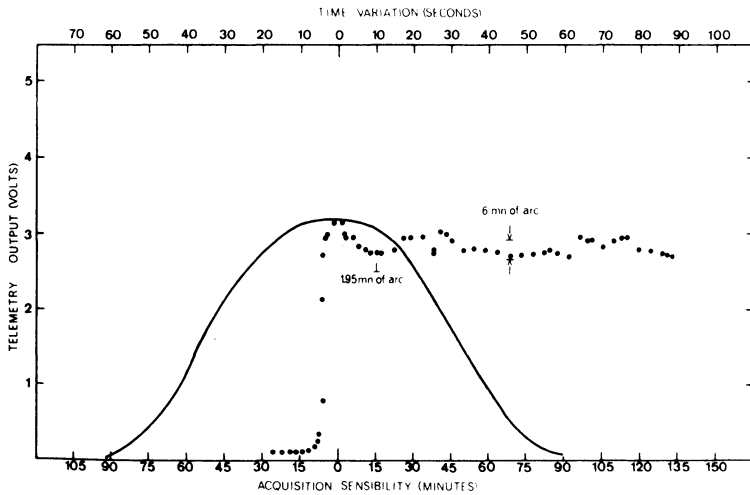


Fig. 13. Variation sensibility of the acquisition.

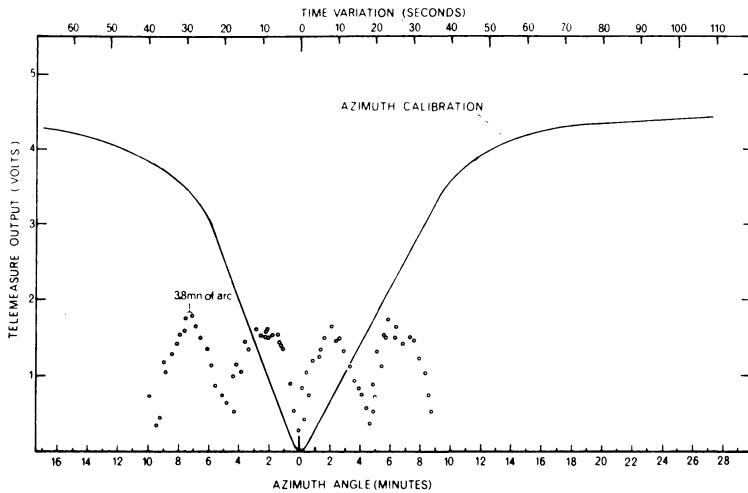


Fig. 14. Variation sensibility of the stabilisation.

which must be carefully selected to provide identical response for each scintillator, is lowered to 0.04 c/s. Compared with the present sensibility which is 2×10^{-5} photons/cm²s keVat 6 mb, we will obtain an increase in the limit sensibility to the value 10^{-6} photons/cm²s keVat 3 mb thanks to an active shielding and a mosaic of detectors just in front of the holes of the collimator.

References

- Bleeker, J. A. M. and Deerenberg, A. J. M.: 1970, *Astrophys. J.* **159**, 215.
 Brini, D., Ciriagi, U., Fuligni, F., and Moretti, E.: 1967, *J. Geophys. Res.* **72**, 903.
 Bui-Van, A. and Vedrenne, G.: 1969, *Nucl. Inst. Meth.* **69**, 303.
 Haymes, R. C., Glenn, S. W., Fishman, G. J., and Harnden, Jr., F. R.: 1969, *J. Geophys. Res.* **74**, 5792.
 Peterson, Laurence E., Jerde, Rod. L., and Jacobson, Allen S.: 1967, *A.I.A.A.J.* **5**, 1921.